Electric Power Systems Research 214 (2023) 108922

Contents lists available at ScienceDirect

Electric Power Systems Research

journal homepage: www.elsevier.com/locate/epsr

Computational intelligence based PEVs aggregator scheduling with support for photovoltaic power penetrated distribution grid under snow conditions

Behzad Hashemi [a], Shamsodin Taheri [a,*], Ana-Maria Cretu [a], Edris Pouresmaeil [b]

[a] Department of Computer Science and Engineering, Université du Québec en Outaouais, Gatineau, QC J8×3×7, Canada
[b] Department of Electrical Engineering and Automation, Aalto University, 00076 Aalto, Espoo, Finland

ARTICLE INFO

Keywords:
Balancing service
Computational intelligence
Distribution system
PEVs aggregator
Photovoltaic plant

ABSTRACT

This paper addresses the issue of optimal day-ahead scheduling of a plug-in electric vehicles (PEVs) aggregator that participates in the electricity market and offers an out-of-market balancing service to the local renewable power penetrated distribution system in a snow-prone area. The proposed balancing service provides a reliable source of flexibility for the extra real-time energy demand of the distribution system operator (DSO) which originates from the difference between its day-ahead bids and the actual demand. The problem is investigated on a snowy day when the DSO's day-ahead decisions encounter more uncertainty due to the considerable effect of snow loss on the DSO's photovoltaic plant performance. The aggregator's scheduling is formulated as two-stage stochastic programming which minimizes the PEVs' charging cost. Monte Carlo simulation and K-means clustering are implemented to generate scenarios of driving patterns and real-time energy market prices, respectively. Offering the balancing service requires day-ahead predictions of the photovoltaic power and the grid load demand which are modeled using long short-term memory networks. The problem is formulated as mixed-integer linear programming. The results show that the proposed scheduling approach reduces the PEVs' charging cost by 53% and guarantees the grid normal operation. Moreover, the balancing service can reduce the expected PEVs' charging cost and the DSO's real-time cost by 12% and 14%, respectively.

1. Introduction

In the past few years, renewable energy resources (RERs), such as solar photovoltaic (PV) systems, and plug-in electric vehicles (PEVs) have attracted much attention to address environmental concerns of global warming. The intermittent nature of RERs together with the uncertain and large charging load of PEVs in high penetration levels demand a highly flexible power grid. This flexibility, however, can be effectively achieved by applying a smart charge and discharge management to the PEVs so that the vehicles are considered not only as controllable loads, that can be shifted to off-peak hours but also as distributed generation units, that can provide technical support for the power grid through the vehicle-to-grid (V2G) technology [1]. This charge-discharge management, which requires the infrastructure of a smart grid, can be performed either in a passive way by the PEV owners with the help of financial incentives, or in an active way by the power grid operators and PEVs aggregators with the aim of reducing the operation cost [2], increasing the profit [3], improving the power grid operation condition [4], reducing the environmental footprints, or a combination of them [5][6]. With the number of PEVs increasing on the road, a competitive market is emerging for PEVs aggregators that, as independent entities, provide smart charging solutions for the PEV owners. This has made the optimal decision-making of a PEVs aggregator an interesting research topic in the past few years [7].

In this context, the optimal day-ahead scheduling of a PEVs aggregator participating in day-ahead electricity markets has been widely addressed in the literature. The day-ahead energy market enables the participants to avoid significant price volatility in the real-time energy market by locking in energy prices before the operating day. Thus, deploying an optimal day-ahead schedule is a vital part of optimizing the operation of an electricity market participant. However, there are uncertain variables that can affect day-ahead schedules. As an example, the availability of PEVs the next day to receive charge/discharge control signals is a source of uncertainty that a PEVs aggregator has to deal with. A well-known and reliable solution to consider the effects of uncertainties in day-ahead decision-making problems is multi-stage stochastic programming where the uncertain variables are modeled as a set

* Corresponding author.
E-mail address: shamsodin.taheri@uqo.ca (S. Taheri).

https://doi.org/10.1016/j.epsr.2022.108922
Received 19 July 2022; Received in revised form 11 October 2022; Accepted 20 October 2022
Available online 26 October 2022
0378-7796/

Nomenclature

Index

d	Plug-in electric vehicle (of set D).
i/j	Grid's node (of set N).
l	Grid's line (of set L).
ll	Segment in linearization (of set LL).
lll	Segment in discretization (of set LLL).
t	Time interval (of set T).
ω	Scenario (of set Ω).

Parameters

A, A'	Auxiliary matrices.
AER	All-electric range of a PEV (km).
c^b, c^L	Battery cost ($/kWh), labor cost for battery replacement ($).
$Cap^{Batt.}$	Battery capacity (kWh).
DOD, L^c	Depth of discharge (unitless), life cycle of a battery (number of charge-discharge cycles).
E	PEV's energy consumption on road (kWh/km).
g, b	Conductance/susceptance of a grid's line (pu).
M	A big constant.
Mil	Trip mileage (km).
$P^{charger}$	Nominal rate of a charger (kW).
Price^{DAM}	Day-ahead energy market prices ($/kWh).
Price^{RTM}	Real-time energy market prices ($/kWh).
r, x	Resistance/reactance of a grid's line (pu).
$SoC^{Final\ Guar.}$	Guaranteed final SoC at the end of the day (%).
SoC^{Arr}, SoC^{LDep}	SoC at arrival/last departure time (%).
$Tariff^{Balancing}$	Price (tariff) of balancing service ($/kWh).
α, $\overline{\beta}$	Slope and length of linear segments.
π_ω	Probability of a scenario.
φ, γ	Risk aversion parameter and confidence level.
η^{ch}	Charge/discharge efficiency.

Variables

Bid^{DAM}	Aggregator's bids in DAM (kW).
Bid^{RTM}	Aggregator's purchases from RTM (kW).
$\mathrm{Cost}^{Batt.\ Deg.}$	Battery degradation cost for all PEVs ($).
Cost^{DAM}	Cost of purchasing energy from DAM ($).
Cost^{RTM}	Cost of purchasing energy from RTM ($).
h, h^+, h^-	Auxiliary binary variables.
P^{ch}, P^{dch}	Charging/discharging power (kW).
P^g, Q^g, P^d, Q^d	Active/reactive power generation/demand (pu).
p^{loss}, q^{loss}	Active/reactive power loss in a grid's line (pu).
p^s, q^s	Active/reactive power flow in a grid's line (pu).
$Pdch^{PEVs}$	Total discharging power of PEVs providing balancing service (kW).
$Ppos^{Balancing}$	DSO's requested balancing power (kW).
$\mathrm{Revenue}^{Balancing}$	Revenue from the balancing service ($).
s, ξ	Risk-associated continuous variables ($).
SoC	State-of-charge of a battery (%).
V, δ	Voltage magnitude/angle of a grid's node (pu).
β^+, β^-	Auxiliary continuous variables.

Abbreviations

CVaR	Conditional value-at-risk.
DAM	Day-ahead energy market.
DAMCPs	Day-ahead energy market clearing prices.
DSO	Distribution system operator.
GHI	Global horizontal irradiance.
LSE	Load serving entity.
LSTM	Long short-term memory.
MILP	Mixed-integer linear programming.
MSEs	Mean squared errors.
PCSs	Public charging stations.
PDF	Probability density function.
PEV	Plug-in electric vehicle.
PV	Photovoltaic.
RERs	Renewable energy resources.
RTC	Real-time cost of DSO.
RTM	Real-time energy market.
RTMCPs	Real-time energy market clearing prices.
TCC	Total charging cost of PEVs.
TOU	Time-of-use.
V2G	Vehicle-to-grid.

of possible scenarios and corrective actions are taken at each stage after the realizations of the scenarios are known [8]. The multi-stage stochastic programming has been implemented in many studies to obtain optimal day-ahead schedules of PEVs aggregators.

In [9], the optimal bidding strategy of a PEVs aggregator participating in the day-ahead and real-time energy markets and the frequency regulation market is modeled as a two-stage stochastic programming approach. It aims at minimizing the aggregator's costs considering the PEV- and market-related scenarios. The authors of [3] investigate the optimal scheduling of a PEVs aggregator bidding in the day-ahead energy and reserve markets. The uncertainties are characterized using two-stage stochastic programming that maximizes the aggregator's profit. A two-stage hierarchical profit-enhancing PEV-aggregation system is proposed in [10] for the day-ahead scheduling and real-time operation of a PEVs aggregator. This approach minimizes the energy consumption cost in electricity markets while enhancing the profits of both PEV owners and energy suppliers. The authors of [11] investigate the day-ahead scheduling of a parking lot aggregator using a three-stage stochastic-based structure by modeling three trading floors of the electricity market including day-ahead, adjustment, and balancing markets. The problem is split into three layers where the electricity market model, parking lot aggregator model, and PEVs model constitute the layers. In [12], a stochastic and dynamically updated two-stage multi-period optimal bidding strategy is developed for a PEVs aggregator. The authors of [13] propose a two-stage programming approach for the day-ahead scheduling of a parking lot aggregator that is developed as a two-level model. It maximizes the aggregator's profit in the first level and minimizes the grid operation cost in the second level. In [14], the day-ahead scheduling of a PEVs aggregator participating in the energy and ancillary service markets is addressed by a two-stage stochastic programming approach. A risk-constrained stochastic approach is proposed in [15] for a PEVs aggregator's optimal participation in day-ahead and reserve markets by involving the risk-related uncertainties through the downside risk constraints. This provides the aggregator with decisions that are made by considering various quantities for risk. Stochastic programming has been widely used for optimal scheduling of PEVs aggregators, however, the published literature either does not consider both the night charging at home and the intraday charging at public charging stations or they do not present a clear methodology for that.

The integration of PEVs into power grids provides a great opportunity to exploit the charge-discharge controllability and flexibility of the vehicles in grid-support services and facilitate higher penetrations of renewable energies in power systems. In this context, PEVs' participation in market-based services, such as reserve or frequency regulation services, has been widely investigated in the literature [16] [7];

however, a limited number of papers address the capabilities of independent PEVs aggregators in providing out-of-market energy services for local distribution grids or other energy entities by investigating the affordability of such services for both sides [17]. These out-of-market services can also be beneficial in case market participation is not achievable for PEVs aggregators due to the market structure or the aggregated PEVs' capacity size. In [18], the day-ahead scheduling of a PEVs aggregator offering balancing services for a wind power producer (WPP) is investigated. The authors of [14] investigate the optimal charging strategy of a PEVs aggregator under the incentive and regulatory policies of the distribution system operator (DSO). The aggregator provides voltage regulation and power loss cost reduction services for the local DSO. The joint operation of a fleet of PEVs with a wind power producer is studied in [19], in which the PEVs aggregator counterbalances WPP fluctuations. In [20], the day-ahead scheduling of a renewable power producer is addressed where the real-time deviations from the day-ahead bids are compensated by demand response and PEVs aggregators. A similar method is proposed in [21] for a wind farm where the formation and scheduling of a virtual power plant by integrating the electric vehicles and flexible loads is investigated. The proposed method aims to minimize the deviation of the wind power generation capacity from the final amount of cleared power in the electricity market. A flexible penalty contract between a PEV charging station and a DSO in terms of voltage security is introduced in [22]. The authors of [23] propose a strategy to provide voltage regulation services by PEVs aggregators for a distribution grid with a grid-connected PV plant. In [4], a coordinated management system is proposed for PEVs that enables the aggregator to offer grid-support services to avoid grid overload and local voltage violation issues. The authors of [24] develop a PEVs aggregator scheduling approach as a bilevel optimization framework that minimizes distribution system congestion. A distributed privacy retaining model for PEVs' charge and discharge management in the presence of distributed generators in a distribution network is proposed in [25] where the network losses reduction, the aggregator's cost minimization, and the distributed generators' profit maximization are considered in a single framework. In [26], an optimal scheduling algorithm for an aggregator based on the benefits of the distribution network, aggregator, and PEV owners is proposed. The algorithm maximizes the aggregator's profit while satisfying the minimum requirements of the demand response capability set by the grid operator and the satisfaction required by the PEV owners. An important design issue in some of the aforementioned services is the lack of a reasonable definition for the interactions between the PEVs aggregators and the service receivers. It is important to note that an independent PEVs aggregator is not responsible for the grid operation condition and providing grid-support services unless it is beneficial for the PEV owners. Considering the potential created by the PEVs' integration into the grid, there is also an opportunity to design new grid-support services to benefit both the aggregator/PEV owners and the grid operator the most and reduce the challenges originating from the intermittency of renewable energy resources, which is investigated in this paper.

One of the sources of uncertainty in day-ahead scheduling problems originates from the intermittent power output of RERs that can be effectively tackled by means of computational intelligence techniques. Using computational intelligence techniques to predict the hourly PV plant power generation has been widely addressed in the literature [27]. In this context, short-term power generation prediction for snow-covered PV panels is more complicated due to the significant effect of snow on the performance of the panels which depends not only on the snow depth but also on snow type, snow cover shape, etc. [28]. Short-term PV power prediction regarding snow-related input variables has been addressed in [29–31], in which an empirical model, a neural network-based model, and a convolutional neural network-based weather classification model are developed, respectively. However, either the results show large errors or no result is presented for snow-covered panels. Other papers such as [32] do not consider snow cover in their models and only refer to the effect of snow as an error in the prediction.

In this paper, the optimal day-ahead scheduling of a PEVs aggregator offering a novel grid-support service is investigated. The proposed service is designed based on the participation profitability, meaning that the aggregator provides the support as far as it is beneficial for the PEV owners. The objective is to minimize the total daily charging cost of the vehicles, by participating in the day-ahead energy market (DAM) and the real-time energy market (RTM), and fulfill the PEV owners' charging demand. This is achieved by developing a two-stage stochastic programming approach to tackle uncertain driving patterns and real-time market clearing prices (RTMCPs). Day-ahead market clearing prices (DAMCPs) can be estimated with high accuracy due to being close to the market clearing process. It is assumed that the local DSO owns a grid-connected PV plant. The DSO's day-ahead predictions of the hourly PV power generation may not be accurate, especially on a snowy day. Snow loss affects the output of PV systems significantly and has a highly uncertain nature. The DSO's inaccurate day-ahead market bids, which originate from errors in day-ahead load and PV power predictions, confront the DSO with the highly volatile RTMCPs. To deal with this issue, a novel local out-of-market balancing service is proposed in this paper which enables the aggregator to provide the extra energy demanded by the grid in real-time and reduce the PEVs' charging costs by the profit earned through the service. Integrating the proposed balancing service into the aggregator's day-ahead scheduling requires day-ahead predictions of the hourly values of the grid load demand and the PV power generation which are obtained by developing two computational intelligence-based predictors. A risk assessment is also performed by integrating the risk-averse equations into the optimization problem. The main contributions of the paper are as follows:

- Proposing a snow loss-aware deep learning-based short-term PV yield predictor using long short-term memory (LSTM) networks to model the hourly power generation of snow-covered PV systems based on meteorological parameters;
- Developing a stochastic programming approach with a comprehensive availability model of PEVs for both residential night-charging and public intraday-charging for optimal day-ahead scheduling of an independent PEVs aggregator;
- Proposing and validating a novel local balancing service offered by the PEVs aggregator to the DSO in order to provide the extra real-time energy demand of the grid by the PEVs and benefit the PEV owners financially.

The rest of the paper is organized as follows. Section 2 discusses the main framework of the problem. The formulation of the proposed approach is presented in Section 3. Section 4 describes the modeling of the uncertain input variables. Case studies and numerical results are investigated in Section 5. Finally, Section 6 is devoted to the conclusion.

2. Main framework

A PEVs aggregator, as an intermediate entity between the PEV owners and the power grid, offers high-tech smart solutions to reduce the charging costs for the PEV owners. This can happen by taking control of the charging or even discharging processes of the vehicles and applying a smart strategy utilizing the smart grid communication infrastructure. In this paper, the optimal day-ahead scheduling of an independent PEVs aggregator providing smart charging solutions for the PEVs in a town in a snow-prone region is investigated. The distribution grid operated by the local DSO is equipped with a large PV plant. The aggregator is assumed to be able to participate in the day-ahead and real-time energy markets through the local DSO in order to provide affordable services for its customers. The direct participation of such a small-scale PEVs aggregator in the market is assumed to be impractical due to the market structure and requirements in terms of the minimum size of the participants. Instead, the aggregator is committed by the local DSO to avoid charging surges and grid overloads due to the simultaneous charging of a large number of PEVs. Such an agreement is beneficial for the aggregator financially and for the DSO technically. This requires the aggregator to adapt its charging policy to the technical limitations of the grid. The main framework of the problem indicating the interactions between all the participants is shown in Fig. 1.

The structure of the energy market is assumed to be similar to that of the New York Independent System Operator (NYISO). The DSO, as a load-serving entity (LSE), can purchase energy by submitting hourly bids to the DAM. Considering the market rules in terms of the minimum size of the participants, the aggregator submits its energy requirements through the local DSO. So, the hourly aggregated values of the grid's net energy demand and the PEVs' charging/discharging power are submitted as the day-ahead bids. The differences in the load consumption of the LSEs as compared to the day-ahead bids are settled at the RTM. Therefore, the DSO has to purchase the extra real-time energy demand (for both the grid and PEVs if there is a difference between the day-ahead bids and the real-time demand) at the RTMCPs.

Before the DAM closure, the aggregator needs to submit its day-ahead hourly energy requests to the DSO. In order to obtain an optimal day-ahead schedule, the aggregator implements a computational intelligence-based approach to minimize its expected cost for the next operating day. Considering the uncertain nature of the driving patterns and energy market prices, the aggregator's decision-making is developed by a two-stage stochastic programming approach [8]. This is a reliable method to address uncertainties by means of probable scenarios of the input variables. The objective is to minimize the charging cost of the vehicles while it is constrained to the satisfaction of the PEV owners in terms of the final battery state of charge (SoC) at the departure time.

From the DSO's viewpoint, the inevitable errors in the day-ahead predictions of the hourly PV power generation (especially for a snowy day) and the hourly load demand of the grid cause inaccuracy in the DSO's day-ahead scheduling. In the case of underestimating the net load of the grid (the aggregated customers' load minus the PV power generation) and a consequent difference between the actual demand and the day-ahead bids, and due to the lack of flexibility, the DSO has to purchase the extra amount of the demanded energy from the RTM. This exposes the DSO to highly volatile RTMCPs. In this condition, the PEVs aggregator is able to provide the extra energy demanded by the grid locally through an out-of-market balancing service which is proposed in this paper. This can happen by manipulating the charging and discharging processes of the vehicles in real-time thanks to the flexibility in the PEVs' charging demand. The aggregator provides this service as far as it is beneficial for the PEV owners in terms of the charging cost. The day-ahead bids of the DSO together with the actual values of the grid load demand and the PV plant power generation determine the extra energy demanded by the DSO in real-time. The proposed balancing service requires the aggregator to consider the uncertain nature of both the grid load demand and the PV power generation as the realization of the probable scenarios in its day-ahead scheduling problem. Before submitting the bids into the DAM, the DSO notifies the aggregator of its bids. Considering the DSO's day-ahead bids, the probable scenarios of the uncertain variables, and the balancing tariff (that the DSO pays to the aggregator for the energy provided by the vehicles in real-time to support the grid), the aggregator submits its optimal decisions for purchasing/selling energy to the DSO. In real-time, the aggregator notifies the DSO of the supported percentage of the grid's energy shortage that can be provided by the vehicles through the balancing service. This local out-of-market service is expected to be a suitable tool for small-scale PEVs aggregators that cannot participate directly in the markets, to reduce the charging costs of their customers, and to ensure a good source of flexibility for the DSO in providing its real-time extra energy demand and avoiding highly fluctuating RTMCPs.

3. Mathematical formulation of the problem

This section presents the mathematical formulation of the aggregator's day-ahead scheduling problem as a two-stage stochastic programming approach. The developed approach consists of two stages, namely here-and-now (the first stage) and wait-and-see (the second stage). Each stage represents a point in time where decisions are made or where uncertainties partially or fully vanish [8]. In the first stage, optimal decisions of purchasing/selling energy from/to the DAM are made before the realization of the scenarios. In the second stage, optimal decisions on (i) the charging/discharging rates of the connected PEVs, (ii) purchasing energy from the RTM, and (iii) providing the balancing service for the DSO, are made after knowing the actual realization of the scenarios. Each decision in the first stage is represented by a single variable, while there are separate variables for each decision in the second stage considering the realization of the scenarios. The inputs of the developed approach are the values of DAMCPs, characteristics of the PEVs, in terms of the battery capacity, nominal charging rate, etc., topology of the grid, and a set of scenarios for each uncertain variable, including RTMCPs, driving patterns, load demand of the grid, and PV plant power generation. Fig. 2 shows the schematic of the proposed two-stage stochastic programming approach in detail. The problem is formulated as a mixed-integer linear programming (MILP) approach. The subscripts d, t, ω, l, and i/j represent PEV, time step, scenario, grid line, and grid node numbers belonging to the sets D, T, Ω, L, and N, respectively. The objective function and the constraints forming the proposed stochastic programming approach are as follows:

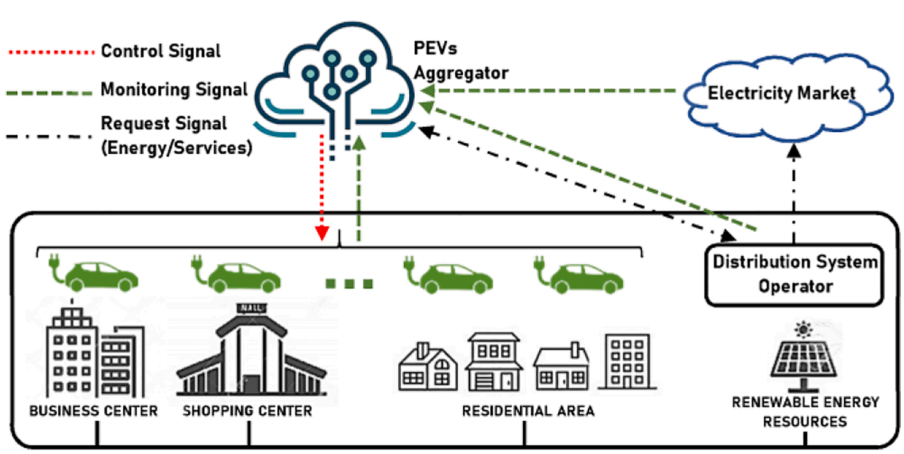

Fig. 1. Main framework of the problem.

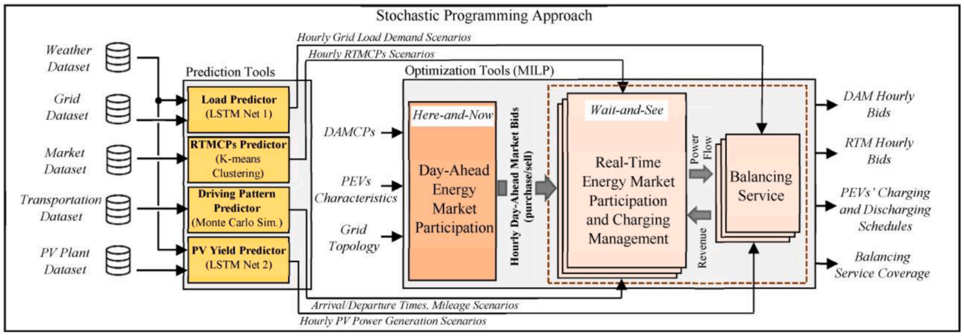

Fig. 2. Structure of the developed stochastic programming approach for the aggregator's day-ahead scheduling.

3.1. Objective function

The objective of the problem is to minimize the expected total daily charging cost of all PEVs. The revenue obtained from providing the proposed balancing service is added to the objective function. The deterministic equivalent of the stochastic programming approach is as follows:

$$MinimizeZ = \text{Cost}^{DAM} + \sum_{\omega=1}^{\Omega} \pi_\omega \times \left[\left(\text{Cost}_\omega^{RTM} + \text{Cost}_\omega^{Batt.Deg.}\right) - \sum_{t=1}^{T} \text{Revenue}_{\omega,t}^{Balancing} \right] \tag{1}$$

where Z is the objective function. Cost^{DAM} and Cost^{RTM} are the costs ($) of purchasing energy from DAM and RTM, respectively. Cost$^{Batt.\ Deg.}$ is the battery degradation cost for all PEVs due to discharging ($). Revenue^{Balancing} is the revenue obtained by providing the proposed balancing service ($). π_ϖ is the probability of each scenario ϖ. The terms of the objective function (Z) are as follows:

- Day-Ahead Market Cost

$$\text{Cost}^{DAM} = \sum_{t=1}^{T} \left(\text{Price}_t^{DAM}\right) \times \text{Bid}_t^{DAM} \tag{2}$$

where Price^{DAM} is DAMCP ($/kWh). Bid^{DAM} is the hourly bid of the aggregator in the DAM. This cost is positive/negative if energy is purchased/sold. The aggregator's bids are added to the DSO's bids and then submitted to the market.

- Real-Time Market Cost

$$\text{Cost}_\omega^{RTM} = \sum_{t=1}^{T} \left(\text{Price}_{\omega,t}^{RTM}\right) \times \text{Bid}_{\omega,t}^{RTM}, \forall\omega \tag{3}$$

where Price^{RTM} is RTMCP ($/kWh). Bid^{RTM} is the aggregator's hourly bid in the RTM. In the case that the aggregator cannot meet its hourly commitment in real-time based on the day-ahead sold energy, this is considered as an increase in the LSE's demand in real-time. So, the RTMCPs should be paid by the aggregator to the RTM through the DSO for this deviation from the commitment. This cost is considered to be always positive because the DSO participates in the market as an LSE and normally submits the major part of its bids in the DAM.

- Battery Degradation Cost

$$\text{Cost}_\omega^{Batt.Deg.} = \sum_{d=1}^{D} \sum_{t=1}^{T} \left(\frac{c^b \times Cap_d^{Batt.} + c^L}{L^c \times Cap_d^{Batt.} \times DoD} \right) \times \frac{P_{\omega,d,t}^{dch}}{\eta^{ch}}, \forall\omega \tag{4}$$

Discharging causes degradation of the batteries and its cost can be calculated based on the discharging power using Eq. (4) [15]. c^b, c^L, L^c, DoD, $Cap^{Batt.}$, η^{ch}, and P^{dch} represent the battery cost ($/kWh), labor cost for replacing the old battery with a new one ($), the life cycle of the battery, depth of discharge, battery capacity, charger efficiency, and the discharging power, respectively.

- Balancing Service

In order to integrate the proposed balancing service to the scheduling problem of the aggregator, a revenue term is added to the objective function that reduces the total charging cost of the PEVs based on the amount of energy they provide for this service. This allows the PEVs to provide part of the extra energy demanded by the DSO in real-time which is beneficial for them based on the structure shown in Fig. 3. The effect of this revenue can be applied later as a reduction to the charging bills of those PEVs participated in the service in the billing calculation process. The following equations form the mechanism of the proposed service.

$$\text{Revenue}_{\omega,t}^{Balancing} \leq \sum_{lll=1}^{LLL} Tariff_{\omega,lll,t}^{Balancing} \times Ppos_{\omega,lll,t}^{Balancing}, \forall\omega, t \tag{5}$$

$$\sum_{d=1}^{D} \left(P_{\omega,d,t}^{dch} - P_{\omega,d,t}^{ch}\right) + \left(\text{Bid}_t^{DAM} + \text{Bid}_{\omega,t}^{RTM}\right) = Pdch_{\omega,t}^{PEVs}, \forall\omega, t \tag{6}$$

$$Pdch_{\omega,t}^{PEVs} = \sum_{lll=1}^{LLL} Ppos_{\omega,lll,t}^{Balancing} - \sum_{lll=1}^{LLL} Pneg_{\omega,lll,t}^{Balancing}, \forall\omega, t \tag{7}$$

$$\text{Bid}_t^{DAM} + \text{Bid}_{\omega,t}^{RTM} \leq \sum_{d=1}^{D} \left(P_{\omega,d,t}^{ch}\right), \forall\omega, t \tag{8}$$

where Revenue^{Balancing} is the revenue obtained by offering the balancing service to the DSO ($). $Ppos^{Balancing}$ is the hourly supplied power by the PEVs into the grid exclusively for the balancing service. $Tariff^{Balancing}$, as the tariff of the service, can be determined using a pricing mechanism

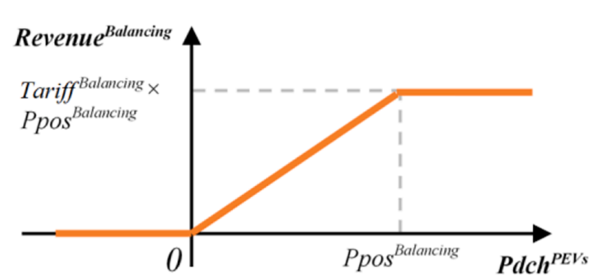

Fig. 3. Structure of the proposed balancing service.

that maximizes the obtained profit by the service. *lll* denotes the segment number for $Pdch^{PEVs}$ in Fig. 3 (here, LLL = 2). The revenue of the balancing service is simply calculated in (5) by multiplying the service tariff by the hourly supplied power by the PEVs into the grid exclusively for this service. In order to be able to calculate this supplied power, the PEVs' market participation is also needed to be considered and distinguished from the PEVs' participation in the service. Moreover, the revenue has to be calculated for the supplied power up to the requested power by the DSO so that $Ppos^{Balancing} \leq$ the requested power by the DSO. These are formulated in Eqs. (6)-(8). The equations needed to divide the values of $Pdch^{PEVs}$ into two segments using auxiliary variables are added to the problem.

3.2. Constraints

The presented objective function is constrained to the following equations.

- Charging and Discharging Rates

$$P^{ch}_{\omega,d,t} \leq P^{charger}_{d} \text{and} P^{dch}_{\omega,d,t} \leq P^{charger}_{d} \times \eta^{ch}, \forall \omega, d, t \tag{9}$$

P^{ch} and P^{dch} are both positive variables and are limited by the nominal charging rate of the battery charger.

- State of Charge Variations

$$SoC_{\omega,d,t} = SoC_{\omega,d,t-1} + \frac{\left(P^{ch}_{\omega,d,t} \times \eta^{ch} - P^{dch}_{\omega,d,t} \Big/ \eta^{ch}\right)}{Cap^{Batt.}_{d}} \times 10^2, \forall \omega, d, t \tag{10}$$

The battery SoC at each hour is determined by the SoC at the previous hour and the energy exchange with the grid, which depends on the charging/discharging power of the battery at that hour.

- State of Charge Bounds

$$20 \leq SoC_{\omega,d,t} \leq 100, \forall \omega, d, t \tag{11}$$

In general, it is recommended to avoid discharging a battery if its SoC is lower than 20% due to battery degradation.

- PEV Owners' Satisfaction in Terms of Final SoC

$$SoC^{Arr}_{\omega,d} + \sum_{t=1}^{T} \frac{\left(P^{ch}_{\omega,d,t} \times \eta^{ch} - P^{dch}_{\omega,d,t} \Big/ \eta^{ch}\right)}{Cap^{Batt.}_{d}} \times 10^2 = SoC^{FinalGuar.}_{\omega,d}, \forall \omega, d \tag{12}$$

This constraint is applied to the vehicles that are connected long enough to the grid to reach the desired SoC. These vehicles will be fully charged and get ready for the next trip. The other vehicles will be charged with a constant charging rate.

- Aggregator's Bids

$$\mathrm{Bid}^{DAM}_{t} + \mathrm{Bid}^{RTM}_{\omega,t} \geq \sum_{d=1}^{D} \left(P^{ch}_{\omega,d,t} - P^{dch}_{\omega,d,t}\right), \forall \omega, t \tag{13}$$

This constraint guarantees that the aggregator's hourly bids meet the total hourly energy demand of the PEVs; so that, the total energy purchased from the DAM and RTM at each hour has to cover the charging load of the vehicles.

- Power Flow Equations

$$\begin{cases} p^{s}_{l,t,\omega} = g_l V_{i,t,\omega} - g_l V_{j,t,\omega} + (1/2) p^{loss}_{l,t,\omega} - b_l \delta_{i,t,\omega} + b_l \delta_{j,t,\omega}; \\ q^{s}_{l,t,\omega} = -b_l V_{i,t,\omega} + b_l V_{j,t,\omega} + (1/2) q^{loss}_{l,t,\omega} - g_l \delta_{i,t,\omega} + g_l \delta_{j,t,\omega}; \end{cases} \forall l, \mathrm{t}, \omega \tag{14}$$

$$\begin{cases} P^{g}_{i,t,\omega} - P^{d}_{i,t,\omega} - \sum_{l \in L} A_{il} \cdot p^{s}_{l,t,\omega} - \sum_{l \in L} A'_{il} \cdot p^{loss}_{l,t,\omega} = 0; \\ Q^{g}_{i,t,\omega} - Q^{d}_{i,t,\omega} - \sum_{l \in L} A_{il} \cdot q^{s}_{l,t,\omega} - \sum_{l \in L} A'_{il} \cdot q^{loss}_{l,t,\omega} + q^{shunt}_{i} = 0; \end{cases} \forall i, \mathrm{t}, \omega \tag{15}$$

$$\begin{cases} p^{loss}_{l,t,\omega} = \left(\left(p^{s}_{l,t,\omega}\right)^2 + \left(q^{s}_{l,t,\omega}\right)^2\right) \times r_l; \\ q^{loss}_{l,t,\omega} = \left(\left(p^{s}_{l,t,\omega}\right)^2 + \left(q^{s}_{l,t,\omega}\right)^2\right) \times x_l; \end{cases} \forall l, \mathrm{t}, \omega \tag{16}$$

The linearized AC power flow model is extracted from [33]. The active-reactive power flows through the grid's lines and the active-reactive power equilibrium in the grid's nodes are formulated in (14) and (15), respectively. Eq. (16), which calculates the active-reactive power losses in the grid's lines based on the flowing power and the resistance-reactance of the lines, will be linearized using the piecewise linear approximation method based on the following set of equations [33].

$$p^{s}_{l,t,\omega} = \sum_{ll=1}^{LL} \beta^{+}_{ll,l,t,\omega} - \sum_{ll=1}^{LL} \beta^{-}_{ll,l,t,\omega}, \forall \mathrm{l}, \mathrm{t}, \omega \tag{17}$$

$$\left(p^{s}_{l,t,\omega}\right)^2 = \sum_{ll=1}^{LL} \alpha_{ll} \times \beta^{+}_{ll,l,t,\omega} + \sum_{ll=1}^{LL} \alpha_{ll} \times \beta^{-}_{ll,l,t,\omega}, \forall \mathrm{l}, \mathrm{t}, \omega \tag{18}$$

$$\left(p^{s}_{l,t,\omega} \Big/ M\right) \leq \mathrm{h}_{l,t,\omega} \leq 1 + \left(p^{s}_{l,t,\omega} \Big/ M\right), \forall \mathrm{l}, \mathrm{t}, \omega \tag{19}$$

$$\begin{cases} 0 \leq \beta^{+}_{ll,l,t,\omega} \leq h_{l,t,\omega} \times \overline{\beta} \\ 0 \leq \beta^{-}_{ll,l,t,\omega} \leq \left(1 - h_{l,t,\omega}\right) \times \overline{\beta} \end{cases}, \forall ll, l, t, \omega \tag{20}$$

$$\begin{cases} \left(\beta^{+}_{ll,l,t,\omega} - \overline{\beta}\right) \Big/ M \leq h^{+}_{ll,l,t,\omega} \leq 1 + \left(\beta^{+}_{ll,l,t,\omega} - \overline{\beta}\right) \Big/ M \\ \left(\beta^{-}_{ll,l,t,\omega} - \overline{\beta}\right) \Big/ M \leq h^{-}_{ll,l,t,\omega} \leq 1 + \left(\beta^{-}_{ll,l,t,\omega} - \overline{\beta}\right) \Big/ M \end{cases}, \forall ll, l, t, \omega \tag{21}$$

$$\begin{cases} \beta^{+}_{ll,l,t,\omega} \leq h^{+}_{ll-1,l,t,\omega} \times \overline{\beta} \\ \beta^{-}_{ll,l,t,\omega} \leq h^{-}_{ll-1,l,t,\omega} \times \overline{\beta} \end{cases}, \forall ll, l, t, \omega \tag{22}$$

Eqs. (19)-(20) and (21-22) guarantee the upper and lower bounds of the linear sections and the connection of the sections, respectively. Similar equations are also used for the reactive power flows.

- Grid Normal Operation Commitment

$$p^{s}_{1,t,\omega} \leq P^{max} \quad , \quad \forall t, \omega \tag{23}$$

As mentioned earlier, the aggregator is committed to maintaining the normal operation of the grid by avoiding the main transformer overload due to the PEVs' charging load. This helps keep the load peak of the grid low and prevents excessive voltage drops in the grid.

3.3. Risk assessment

Despite the aforementioned risk-neutral decision-making formulation, a risk assessment using the popular conditional value-at-risk (CVaR) as the risk measure is performed to evaluate the proposed approach considering the risk of variability associated with the aggregator's cost [8]. The objective function of the risk-averse approach is defined in Eq. (24). All the constraints of the risk-neutral formulation together with Eqs. (25) and (26) constitute the new optimization problem.

$$Min.Z^{risk-averse} = (1-\varphi) \times Z + \varphi \times \left(\left(\frac{1}{1-\gamma} \right) \sum_{\omega=1}^{\Omega} \pi_\omega \times s_\omega - \xi \right) \tag{24}$$

$$\begin{aligned} &\text{Cost}^{DAM} + \text{Cost}_\omega^{RTM} + \text{Cost}_\omega^{Batt.Deg.} - \\ &\sum_{t=1}^{T} \text{Revenue}_{\omega,t}^{Balancing} + \xi \le s_\omega, \forall \omega \in \Omega \end{aligned} \tag{25}$$

$$s_\omega \ge 0, \forall \omega \in \Omega \tag{26}$$

4. Modeling of uncertain input variables

Concerning the aggregator's scheduling as a stochastic programming approach, two scenario generation methods for driving patterns and RTMCPs are presented. Considering the proposed balancing service, two predictors for the load demand of the grid and PV power generation are proposed. The data used for the modeling is available in: https://drive.google.com/file/d/1d8oIxLk8y-4n8L6MjzCbaatXLd5pkLPa/view.

4.1. Driving patterns of PEV owners

The uncertain driving patterns can be modeled by three attributes namely the arrival and departure times (when a PEV arrives/departs at/from a charging station), and the daily mileage (total distance a PEV travels on a day). All PEVs can get connected to the grid through residential chargers and some are randomly selected to get connected in public charging stations (PCSs) during the day. Two types of PCSs, i.e. business center PCSs and shopping center PCSs, are considered. The arrival and departure times of the PEVs are generated randomly based on the widely used normal probability density functions (pdfs). Daily mileages are generated using a Lognormal pdf. The parameters of the pdfs for each type of charging station are presented in Table 1.

The stochastic driving patterns are generated using a Monte Carlo simulation based on the proposed flowchart shown in Fig. 4. At first, arrival and departure times at/from home are generated for all vehicles. Then based on the number, type, and capacity of the PCSs, some PEVs are randomly selected to get charged at PCSs. The arrival and departure times of the selected PEVs at/from the PCSs are finally generated considering the previously generated arrival and departure times.

The state of charge (SoC) of a PEV's battery at its arrival time is calculated based on the generated driving patterns:

$$SoC^{Arr} = \begin{cases} SoC^{LDep} - \dfrac{Mil \times E}{Cap^{Batt.}} \times 100, Mil < 0.8AER \\ 20\%, Mil > 0.8AER \end{cases} \tag{27}$$

Table 1
Parameters of pdfs related to driving patterns.

Station	Residential		Business PCSs		Shopping PCSs		Daily
Parameter	Arr. Time	Dep. Time	Arr. Time	Dep. Time	Arr. Time	Dep. Time	Mileage
Mean	20	7.5	8.5	14	16	18	3.715
Stand. Dev.	1.5	0.75	0.5	0.5	1	1	0.6

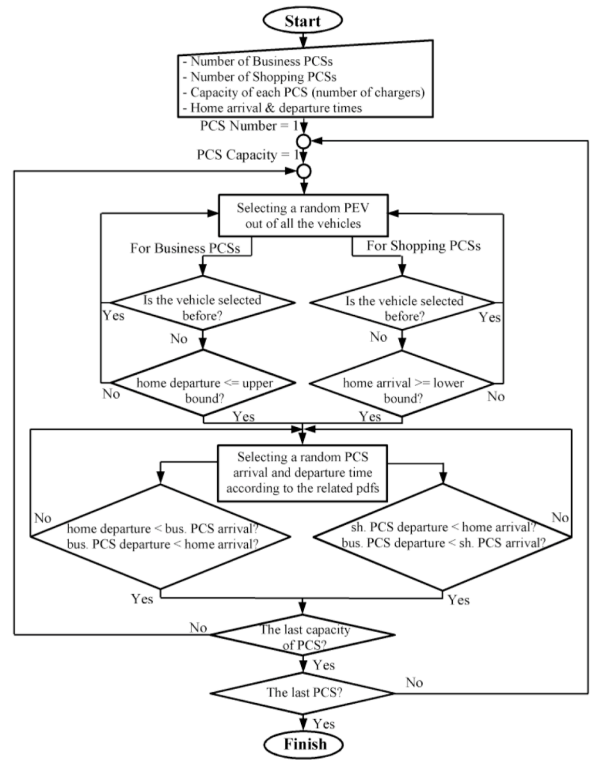

Fig. 4. Flowchart of stochastic driving patterns of PEV owners.

4.2. Real-Time market clearing prices (RTMCPs)

Considering the participation of the aggregator in the RTM, the probable scenarios of RTMCPs should be integrated into the problem. The RTMCPs are normally highly volatile since they depend on many factors including the uncertain behavior of the market participants. Thus, K-means clustering is implemented to generate the scenarios based on K centroids of the clusters over historical data. The probability of each scenario is calculated based on the number of members of each cluster. This method enables the aggregator to consider all various probable RTMCP patterns in a historical dataset.

The historical data of the NYISO is used for this purpose [34]. A one-time market clearing process at the beginning of the 24-hour scheduling horizon is considered to reduce complexity. 23 Feb. 2015, which is a winter day, is arbitrarily chosen as the operating day. The hourly RTMCPs for 15 days before that date constitute the dataset and 5-means clustering is applied to that.

4.3. Load demand of the grid

Integrating the proposed balancing service to the scheduling problem of the aggregator demands day-ahead predictions of the hourly load demand of the grid which are obtained here using a computational intelligence technique. In order to provide real historical data on the hourly load demand of a town, a dataset corresponding to the city of Dayton, Ohio is extracted [35] which was the closest city to New York with a publicly available dataset. 23 Feb. 2015 (Monday) is chosen as the operating day. Considering the periodic patterns in the load demand of the grid, its high correlation with ambient temperature, days of the week, and months of the year, and its lower uncertainty compared to other uncertain input variables in this study, the load demand prediction model is built based on a historical data containing the most similar data points to the operating day. This enables us to build a model faster with the most relevant data in a smaller dataset. In this way, the model can be rebuilt for each operating day by shifting the dataset by one day. To this end, the data for 30 days before the operating day, and 30 days before and 30 days after the same date in the previous year (2014) constitute the dataset that covers measurements over 3 months. The hourly values of ambient temperature are extracted for the city of Dayton [36]. The attribute and target variables are:

- Att. 1: Weekday/weekend numbers (1 for Monday to 7 for Sunday);
- Att. 2: Hours (1 to 24);
- Att. 3: Temperature;
- Target: Hourly load demand of the grid.

The line graphs of the load and temperature in the dataset are shown in Fig. 5. Considering the nature of the data as time series, Long Short-Term Memory (LSTM) network, as a recurrent deep learning model, is used to build the load demand predictor [37] which can capture long-term dependencies in the data. The first 2016 data points (84 days) are used to train the model and the next 168 data points (the next 7 days) are used as the validation set. Bayesian optimization is implemented to select optimal hyperparameters based on the validation set. Then, the model is used to make a prediction on the unseen data of the operating day. The mean squared errors (MSEs) together with the optimal hyperparameters of the model are presented in Table 2. The line graphs of the real and predicted normalized values of the target variable on the validation set and the test set are shown in Figs. 6(a) and 6(b), respectively. The MSE value on the test set is 0.00204. The figures demonstrate the ability of the model to predict the load demand of the grid.

4.4. PV power generation

Another source of uncertainty considering the proposed balancing service originates from the PV plant. PV yield prediction can be even more challenging on a snowy day, not only due to the errors in the day-ahead predictions of the meteorological parameters but also because of the complexity of obtaining the exact values of the power generation for snow-covered PV panels. Snow loss can be very large and variable depending on several factors such as the snow depth, the type of snow, the shape of the snow cover, etc. Therefore, a computational intelligence-based snow loss-aware PV power generation predictor is built that allows the aggregator to consider all probable scenarios for the next snowy day.

Historical data of the hourly PV yield and the meteorological parameters are extracted for a PV system in New York [38]. A snowy winter day (17 Feb. 2015) is chosen as the operating day. Considering the periodic patterns in the power generation of a PV system over years and due to the significant dependence of the PV power on weather conditions and meteorological parameters, the PV power prediction model in this paper is built based on historical data containing data points in the most similar weather conditions to the operating day. To this end, the data of 30 days before the operating date, and 30 days before and 30 days after the similar date in the past year (17 Feb. 2014)

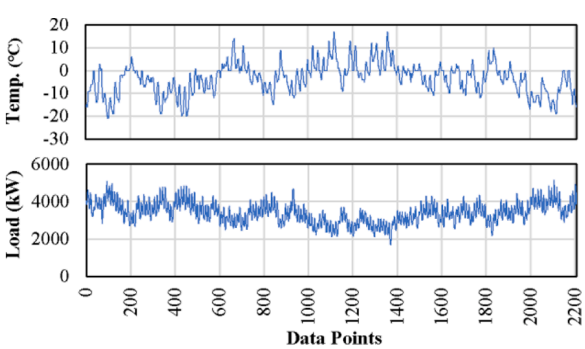

Fig. 5. Line graphs of the load demand and temperature in the historical dataset of the load demand predictor.

and the past 2 years (17 Feb. 2013) are selected to constitute the dataset, which covers measurements over 5 months. This approach to building the dataset has been validated after training models based on datasets with different sizes and comparing their performance. Since the data is gathered over three consecutive years, the annual trend, such as the effect of increasing system power losses, is also maintained. The attribute and target variables are:

- Att. 1: Hours of the day (1 to 24);
- Att. 2: Hourly ambient temperature;
- Att. 3: Hourly global horizontal irradiance (GHI);
- Att. 4: Daily snowfall;
- Att. 5: Daily snow depth;
- Target: Hourly PV power generation.

The line graphs of the electrical and meteorological parameters in the dataset are shown in Fig. 7. The last 24 data points (the last day) are used as the test set. 720 data points (30 days) before the operating day are used as the validation set. The first 2928 data points (122 days) are used as the training set. The LSTM network together with the Bayesian optimization is implemented to build the optimal model. Then, the model is used to make a prediction on the unseen data of the operating day in the test set. The mean squared errors (MSEs) together with the optimal hyperparameters of the model are presented in Table 2. The line graphs of the real and predicted normalized values of the target variable on the validation set and the test set are shown in Figs. 8(a) and 8(b), respectively. The MSE value on the test set is 0.00055.

5. Case studies and numerical results

The topology of the 20.8 kV distribution grid, where PEVs are distributed, is adapted from the IEEE 34-node test system [39]. The main feeder is connected to the upstream grid by a 5.5 MW transformer. Three business PCSs (connected to nodes 5, 10, and 19) and two shopping PCSs (connected to nodes 14 and 18) are considered in the grid. Personal residential chargers are connected to the other nodes (except nodes 1 and 24). A 2.3 MW PV plant owned by the DSO is connected to node 24.

In order to generate the scenarios of the hourly PV power generation and the hourly load demand of the grid, 1000 scenarios of each uncertain attribute variable including temperature, GHI, snowfall, and snow depth are generated by adding a random value from a normal distribution to the real recorded values on the operating day. It is assumed that the predicted values of temperature are more accurate for the first hours of the day (± 1 °C) compared to the last hours (± 4 °C). Moreover, the variations of the hourly GHI at noon (± 200 W/m^2) are assumed to be bigger than the variations after sunrise or before sunset (± 50 W/m^2). It is also assumed that the values of daily snowfall may change between 0 and 15 cm. The snow depth can be simply calculated based on the snowfall and the snow depth on the previous day. The real values together with 1000 generated scenarios of these parameters are shown in Fig. 9. These scenarios are fed into the models and 1000 scenarios of the hourly PV power generation and the hourly load demand are generated. Then, a scenario reduction procedure based on Kantorovich distance is implemented to reduce the number of scenarios to lower the computational burden. Finally, the 5 most probable scenarios are selected and shown in Fig. 10.

Eight different types of PEVs are considered [40]. Table 3 presents the properties of the PEVs. The penetration level of PEVs is defined as the ratio of the number of consumers with a PEV to the total number of consumers in the grid. Considering the residential load, the coincidence factor, and the average load peak of a consumer, the number of PEVs at the penetration level of 40% is 1000. The Roulette Wheel Mechanism is used to locate the PEV owners' houses randomly among the residential nodes. Moreover, 70 vehicles are randomly selected to be charged in each PCSs.

Finally, 25 final scenarios are formed by combining each RTMCPs

Table 2
Parameters of the grid load demand and PV yield predictors.

Model	Validation MSE	Test MSE	Num. of Hidden Units	Initial Learning Rate	Learning Rate Drop Period	Learning Rate Drop Factor	Maximum Epochs	Mini-Batch Size
Load Predictor (LSTM Net 1)	0.00214	0.00204	34	0.1	97	0.5	589	9
PV Predictor (LSTM Net 2)	0.00409	0.00055	87	0.1	100	0.5	75	48

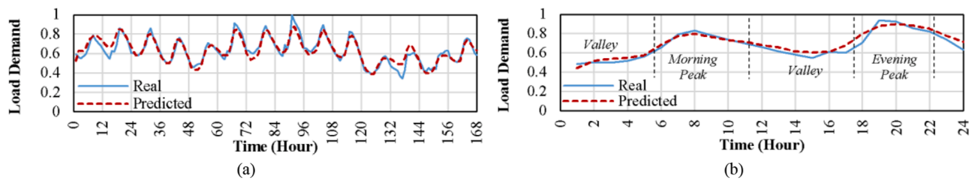

Fig. 6. The real and predicted values of the hourly load demand using the LSTM model on (a) the validation set and (b) the test set.

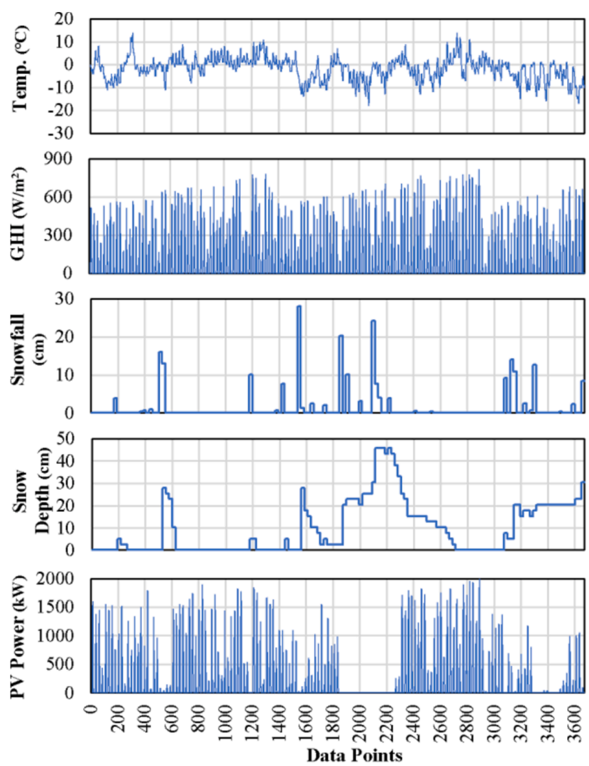

Fig. 7. Line graphs of the electrical and meteorological parameters in the historical dataset of the PV yield predictor.

scenario with five scenarios of the other three uncertain input variables. The proposed MILP problem is solved using the CPLEX solver in GAMS software. Five cases are studied to prove the effectiveness of the proposed approach.

5.1. Cases 1 and 2: Uncoordinated and off-peak charging

The PEV owners plug in their vehicles as soon as they arrive home. In the uncoordinated charging mode, charging starts immediately with the maximum charging rate until the battery is fully charged (charging up to 90% of SoC is assumed, regarding the linear section of the charging curve, if the PEV is plugged in long enough). Time-of-Use (TOU) tariffs of the DSO are used to calculate the charging costs. In the off-peak charging mode, the charging process is delayed until midnight since the lower step of the TOU tariffs starts at 12 a.m. The charging bills also include a fixed monthly fee for a separate meter. In the winter of 2015, electricity consumers in New York paid a monthly fee of 19.87 $ and 1.36 cents (1:00 to 7:00)–7.13 cents (8:00 to 24:00) for every kWh energy consumed [34].

The expected hourly charging load of all PEVs together with the expected hourly load demand of the grid, the expected hourly voltage magnitude of the last node (node 34), and the arrival and departure SoCs of the vehicles are shown in Fig. 11.

In case 1, the PEVs' charging load peaks at 8 p.m. when most vehicles are coming back home and it has a gradual increase. This peak in case 2 happens at 1 a.m. and is more than three times bigger than that in case 1. As a result, the voltage drop at node 34 in case 2 is more severe compared to case 1; however, its duration is longer in case 1. Hence, a voltage drop across the last nodes of the feeder and the overload of the main feeder transformer at peak hours are undesirable consequences of the uncoordinated and off-peak charging of a large number of PEVs. The extra load incurred by the business and shopping PCSs to the grid during the day is not significant since the vehicles are mainly getting fully charged at home. Moreover, the majority of the PEVs have been charged to the predefined 90% of SoC.

The expected daily charging costs of all PEVs in cases 1 and 2 are 1301 $ and 867 $, respectively. Thus, off-peak charging is more beneficial for PEV owners since a major part of the charging process occurs at the lowest level of the TOU tariff; however, the grid experiences worse technical challenges in this case.

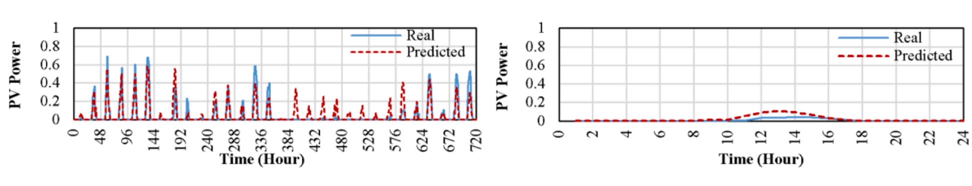

Fig. 8. The real and predicted values of the hourly PV power generation using the LSTM model on (a) the validation set and (b) the test set.

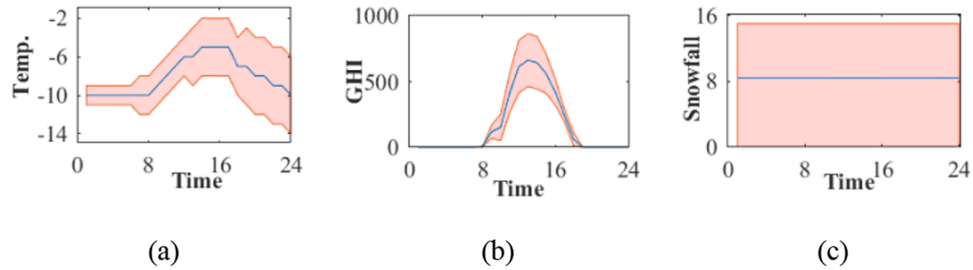

Fig. 9. Real values (blue line) and 1000 generated scenarios of (a) hourly temperature, (b) hourly GHI, and (c) daily snowfall.

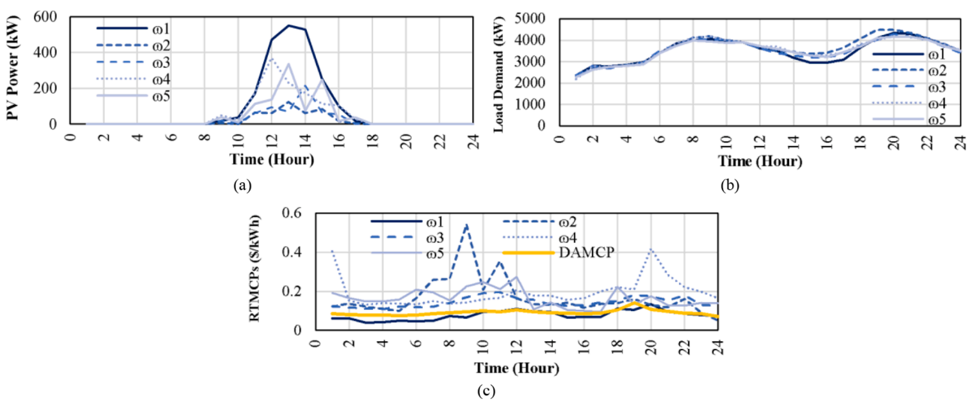

Fig. 10. Scenarios of (a) PV power, (b) load demand, and (c) RTMCPs.

Table 3
Properties of the PEVs.

PEV Type Number	1	2	3	4	5	6	7	8
Battery Capacity (kWh)	100	80	60	40	20	15	10	5
All Electric Range (km)	490	450	320	220	110	75	45	23
Market Share (%)	13	58	6	5	4	2	9	3
Charger Rate (kW)	11.5	11.5	7.2	6.6	6.6	6.6	3.3	3.3

5.2. Case 3: coordinated charging (the basic model)

In this section, the developed stochastic programming approach (without the balancing service) is investigated. The results have been obtained considering the expected price of brand-new batteries in 2023 [41] and are shown in Fig. 12. The major part of the charging load has been shifted to the off-peak hours when the price of energy in the market is lower. This shows the significant effect of the DAMCPs on the established schedule of the aggregator for the next operating day. Unlike cases 1 and 2, the resulting load shift avoids both main feeder overloads and voltage drops lower than 0.95 p.u. across the grid (Figs. 12(a) and 12(b)) by distributing the charging load of the vehicles over six hours, obtained by the aggregator's commitment to prevent charging surges. Moreover, PEVs have being discharged at 7 p.m. when DAMCP is higher. This reduces the overall charging cost of the vehicles by contributing to load serving at peak hours. Considering the highly uncertain RTMCPs, it is clear in Fig. 12(c) that the aggregator tends to provide the major part of the PEVs' energy demand from DAM to guarantee a minimum expected charging cost for the next operating day. As can be seen in Fig. 12 (d), up to 530 kWh of the daily charging demand has been purchased from the RTM at hours with lower RTMCPs in each scenario while in

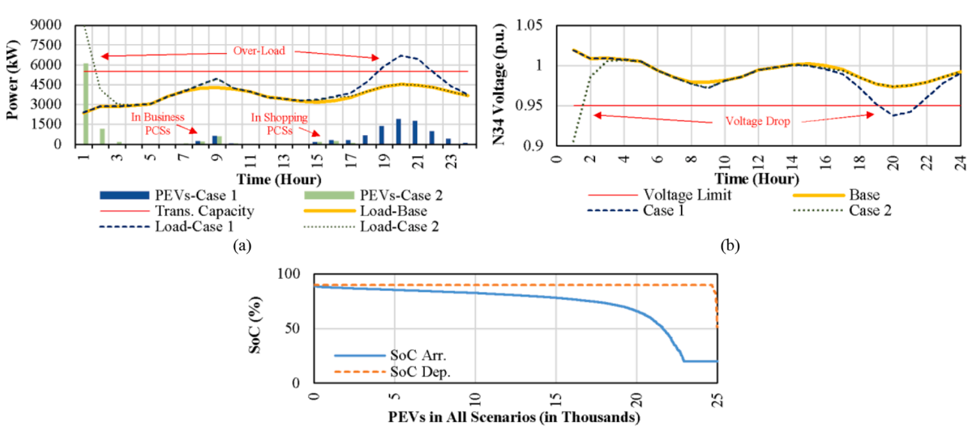

Fig. 11. Case 1 and case 2 results: (a) Expected charging and main feeder load, (b) expected voltage magnitude of node 34, and (c) arrival and departure battery SoCs.

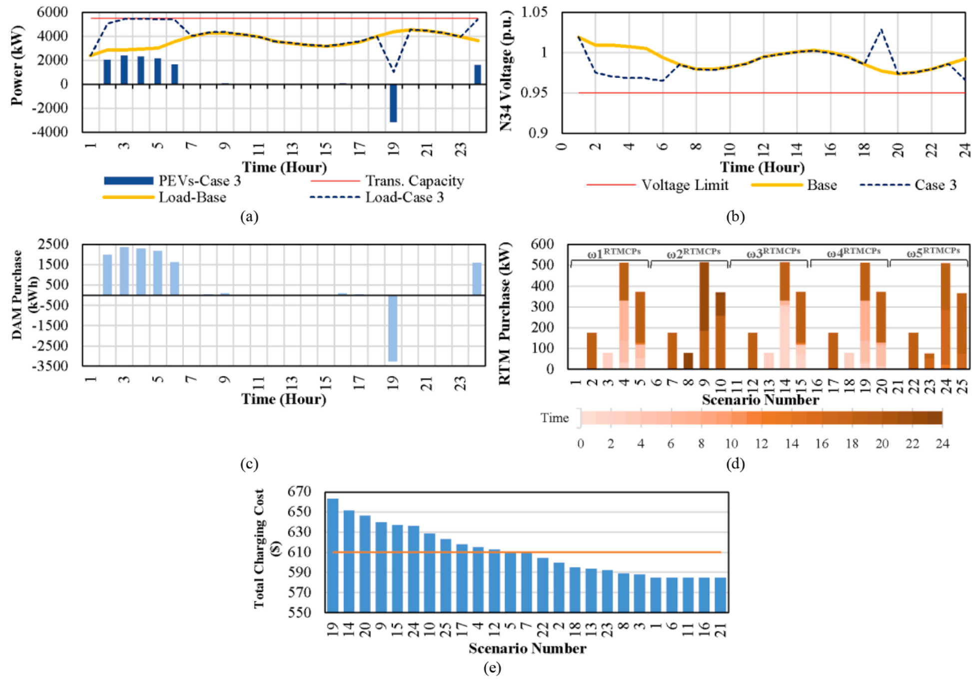

Fig. 12. Case 3 results: (a) Expected charging power and main feeder load, (b) expected voltage magnitude of node 34, (c) aggregator's DAM energy purchases, (d) aggregator's RTM energy purchases, and (e) total charging cost in each scenario.

scenarios 1, 6, 11, 16, and 21, almost all the charging demand of the PEVs has been purchased from DAM. The difference in the RTM purchase values for every five consecutive scenarios in Fig. 12(d) originates from the difference in the driving patterns and consequently the charging requirements.

As indicated in Fig. 12(e), the expected daily charging cost of all PEVs is 610 $ (53% lower than case 1 and 30% lower than case 2), ranging from 663 $ in scenario 19 to 584 $ in scenario 21. The aggregator's cost in DAM (purchases minus sells) and its expected cost in RTM are 497 $ and 28 $, respectively. The expected degradation cost of all batteries is 85 $. The aggregated discharging power in Fig. 12(a) shows that the vehicle-to-grid (V2G) is affordable only when the price of energy is high enough to compensate for the battery degradation cost and charging/discharging power losses. So, batteries' technology improvement and price reduction can play a key role in making V2G services more affordable and popular. In general, the coordinated charging approach can reduce the charging cost of PEVs compared to the uncoordinated and off-peak charging and at the same time, guarantee the normal operation of the grid.

5.3. Case 4: Coordinated charging with balancing service

The aggregator's day-ahead scheduling with the proposed balancing service is investigated in case 4. A pricing mechanism is used to calculate $Tariff^{Balancing}$ in Eq. (5) as a multiple of RTMCP unless RTMCP is higher than a particular threshold. This prevents the reflection of the surges and large values of RTMCPs in $Tariff^{Balancing}$. This threshold can be considered as a multiple of DAMCP and used as a cap for $Tariff^{Balancing}$. Moreover, due to the highly downward trend in the prices of brand-new batteries, two cases of ½ battery prices (0.5*BP) and without battery degradation cost (0*BP) are also investigated.

The DSO's hourly balancing service requests for the first 5 scenarios are shown in Fig. 13(a) which reflects the effect of the combination of 5 PV yield scenarios and 5 grid load demand scenarios. The peak and the largest variability of the requests happened at noon when the PV plant may not be able to supply the grid as expected in the snow conditions. The expected value of the total charging cost (TCC) reduction for the PEVs together with the DSO's real-time cost (RTC), as the sum of the costs of the balancing service and the purchase of the remaining amount of the demand from the RTM, reduction thanks to the balancing service

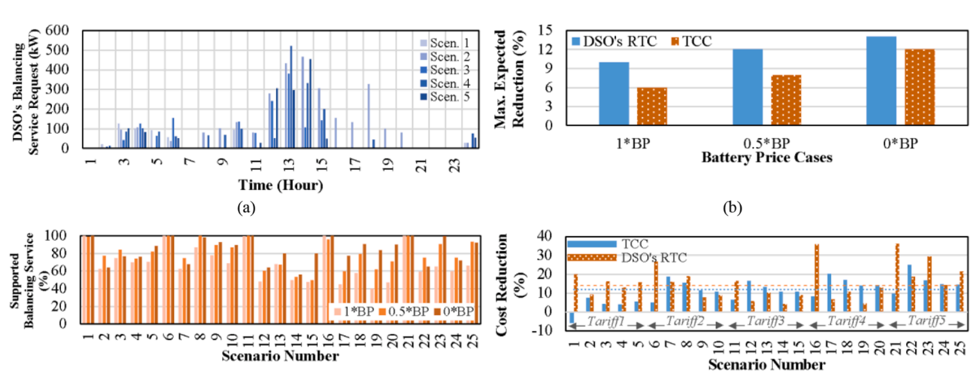

Fig. 13. Case 4 results: (a) DSO's balancing service requests, (b) maximum expected TCC and DSO's RTC reductions, (c) supported balancing service, and (d) TCC and DSO's RTC reductions in the case of ignoring the battery degradation cost.

compared to case 3 are shown for three cases of battery prices in Fig. 13(b). A grid search has been performed to find the best $Tariff^{Balancing}$ to maximize the expected value of the aforementioned reductions. The maximum expected DSO's RTC reduction can be achieved by $Tariff^{Balancing} = 1.1\times$RTMCPs and $1.9\times$DAMCPs as a cap and the maximum expected TCC reduction can be achieved by $Tariff^{Balancing} = 0.8\times$RTMCPs and $1.3\times$DAMCPs as a cap. As can be seen in Fig. 13(b), decreasing the battery prices can increase the benefit obtained by implementing the balancing service where a 14% reduction in the DSO's RTC and a 12% reduction in the PEVs' TCC have been obtained. This is achieved by a higher contribution of the PEVs to support the balancing requests, from an average of 70% in the case of 1*BP to an average of 85% in the case of 0*BP, which is indicated in Fig. 13(c). Smaller DSO's balancing requests have resulted in almost complete support of the balancing service by the PEVs in scenarios 1, 6, 11, 16, and 21. The percentage of TCC and DSO's RTC reductions in the case of 0*BP for each scenario together with their expected values (horizontal dash lines) are shown in Fig. 13(d). The maximum and the minimum reductions have been obtained in scenarios 21–25 and 11–15 using $Tariff^{Balancing}$ based on the fifth and the third scenarios of RTMCPs, respectively. As can be seen in the results of this case, implementing the proposed local balancing service can be beneficial for both the DSO and the PEVs aggregator. In fact, this type of grid-support service can enable small-scale aggregators to contribute to facilitating the higher penetrations of intermittent renewable energies in local power grids. Similar to case 3, the normal operation of the grid has been obtained based on the aggregator's schedule by avoiding the charging surges over the operating day.

5.4. Case 5: Risk-averse coordinated charging with balancing service

In this case, the results of the risk-averse formulation based on Eqs. (24)-(26) are investigated. To this end, the battery degradation cost is fully considered (battery price case of 1*BP), $Tariff^{Balancing}$ is set to have the most expected TCC reduction, and the confidence level (γ), which categorizes high-cost and low-cost scenarios, is set as 0.9. The cumulative distribution functions for three cases of the weighting parameter φ, which materializes the trade-off between the expected cost and the risk aversion, are illustrated in Fig. 14(a).

As can be seen, the expected TCC and CVaR, which denotes the expected cost of the worst scenarios, in the risk-neutral formulation (with φ=0) are 578 $ and 625$, respectively. As expected, considering the risk measure and increasing its weight increases the expected cost and reduces the CVaR; so that, with φ=1, they are very close to each other (expected cost=616 $ and CVaR=617 $). So, the risk-averse formulation has reduced the cost of encountering the worse scenarios at the expense of increasing the expected TCC. As can be seen in Fig. 14(b) for risk-averse results with φ=1 and γ=0.9, the PEVs have less supported the balancing service requests in most of the scenarios after considering the risk in the optimization problem. A sensitivity analysis is also performed for different values of the confidence level (γ) from 0.5 to 0.99 with φ=1. The results are shown in Fig. 14(c). The confidence level plays an important role in capturing the adverse effect of the worst scenarios. By increasing the confidence level, the expected total charging cost will rely on a fewer number of high-cost scenarios ((1- γ)$\times$100%). Therefore, the expected cost and the CVaR both have increased by raising the confidence level.

In general, the results prove the effectiveness of the proposed computational intelligence-based scheduling approach in reducing the charging cost of the PEVs and maintaining the normal operation of the grid compared to the un- or semi-coordinated approaches. Moreover, the integrated out-of-market balancing service is proved to be a useful tool for reducing the challenges that a grid operator deals with in high penetrations of intermittent renewable energies and to be beneficial for the aggregator/PEV owners. To clarify the differences between the case studies, a brief benchmarking is performed in Table 4, in which the levels of achievements are ranked from low (*) to high (***). As can be observed, the developed stochastic programming approach with the proposed balancing service (cases 4 and 5) is the most desirable from different aspects.

6. Conclusion

This paper addresses the issue of day-ahead scheduling of a PEVs aggregator that participates in both day-ahead and real-time energy markets on behalf of the PEV owners through the local DSO. The aggregator can also provide the DSO's extra energy demand in real-time, which originates from the differences between the DSO's day-ahead bids and the actual load demand of the renewable power penetrated

Table 4
Benchmark.

	Case 1	Case 2	Case 3	Case 4	Case 5
PEV Owners' Satisfaction (E. Range)	***	***	***	***	***
PEVs' Charging Costs Reduction	–	*	**	***	***
Guarantee Grid Reliability (Overload)	–	–	***	***	***
DSO's Operation Cost Reduction	–	*	**	***	***
Risk Aversion Scheduling	–	–	–	–	***

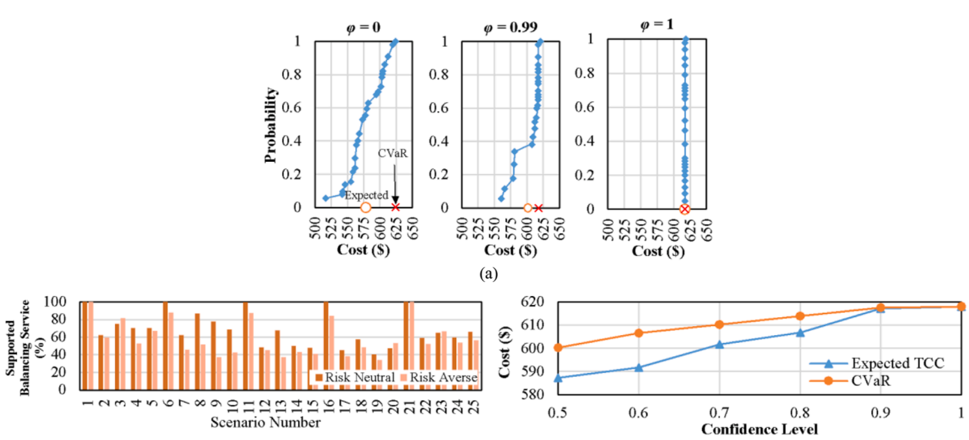

Fig. 14. Case 5 results: (a) Cumulative distribution function for risk-neutral and risk-averse approaches, (b) supported balancing service with risk-neutral and risk-averse formulations, and (c) the effect of confidence level on CVaR and expected TCC.

distribution system, through a proposed out-of-market balancing service, and reduce the charging costs of the vehicles. A two-stage stochastic approach with a comprehensive availability model of PEVs for both residential night-charging and public intraday-charging has been developed that minimizes the total charging cost of the PEVs. Computational intelligence methods have been used to model the uncertain input variables on a snowy day and generate the scenarios. The results show that the proposed day-ahead scheduling approach can reduce the expected total charging cost by 53% and 30% compared to the uncoordinated and off-peak charging modes, respectively. It also guarantees the normal operation of the grid. Moreover, the proposed balancing service can be beneficial for both the DSO and the PEV owners. Depending on the price of the service and brand-new batteries, it can reduce up to 25% of the total charging cost and 36% of the DSO's real-time cost while the expected reductions are 12% and 14% compared to the same condition without the service, respectively. Moreover, the risk-averse formulation can reduce the cost of encountering the worst scenarios while it increases the expected charging cost significantly.

CRediT authorship contribution statement

Behzad Hashemi: Software, Methodology, Validation, Writing – original draft. **Shamsodin Taheri:** Conceptualization, Methodology, Writing – review & editing, Supervision. **Ana-Maria Cretu:** Conceptualization, Methodology, Writing – review & editing, Supervision. **Edris Pouresmaeil:** Methodology, Writing – review & editing.

Declaration of Competing Interest

The authors declare that they have no known competing financial interests or personal relationships that could have appeared to influence the work reported in this paper.

Data availability

The data that has been used is confidential.

Acknowledgments

The authors would like to thank NSERC for financial support, which made this research possible.

References

[1] T.U. Solanke, V.K. Ramachandaramurthy, J.Y. Yong, J. Pasupuleti, P. Kasinathan, A. Rajagopalan, A review of strategic charging–discharging control of grid-connected electric vehicles, J. Energy Storage 28 (Apr. 2020).
[2] Q. Huang, X. Wang, J. Fan, S. Qi, W. Zhang, C. Zhu, V2G optimal scheduling of multiple EV aggregator based on TOU electricity price, in: 2019 IEEE Int. Conf. Environ. Electr. Eng. - 2019 IEEE Ind. Commer. Power Syst. Europe, EEEIC /I&CPS Europe, June 2019, pp. 1–6.
[3] M. Alipour, B. Mohammadi-Ivatloo, M. Moradi-Dalvand, K. Zare, Stochastic scheduling of aggregators of plug-in electric vehicles for participation in energy and ancillary service markets, Energy 118 (Jan. 2017) 1168–1179.
[4] M.S.H. Nizami, M.J. Hossain, K. Mahmud, A coordinated electric vehicle management system for grid-support services in residential networks, IEEE Syst. J. 15 (2) (June 2021) 2066–2077.
[5] H. Shahinzadeh, J. Moradi, M. Longo, W. Yaïci, and S. Azani, "Integration of parking lot capacity in retail energy and reserve market mechanism," in *10th Int. Conf. Smart Grid (icSmartGrid)*, June 2022, pp. 275–279.
[6] L. Bagherzadeh, H. Shahinzadeh, and G.B. Gharehpetian, "Scheduling of distributed energy resources in active distribution networks considering combination of techno-economic and environmental objectives," in *2019 Int. Power Syst. Conf. (PSC)*, Dec. 2019, pp. 687–695.
[7] S. Kerscher, P. Arboleya, The key role of aggregators in the energy transition under the latest European regulatory framework, Int. J. Electr. Power Energy Syst. 134 (Jan. 2022).
[8] A.J. Conejo, M. Carrion, J.M. Morales, Decision Making Under Uncertainty in Electricity Markets, 1, Springer, New Year, 2010.
[9] R. Habibifar, A.A. Lekvan, M. Ehsan, A risk-constrained decision support tool for EV aggregators participating in energy and frequency regulation markets, Electr. Power Syst. Res. 185 (Aug. 2020).
[10] U. ur Rehman, M. Riaz, M.Y. Wani, A robust optimization method for optimizing day-ahead operation of the electric vehicles aggregator, Int. J. Electr. Power Energy Syst. 132 (Nov. 2021).
[11] M.K. Daryabari, R. Keypour, H. Golmohamadi, Stochastic energy management of responsive plug-in electric vehicles characterizing parking lot aggregators, Appl. Energy 279 (Dec. 2020).
[12] Y. Vardanyan, H. Madsen, Optimal coordinated bidding of a profit maximizing, risk-averse EV aggregator in three-settlement markets under uncertainty, Energies 12 (9) (May 2019).
[13] M. Shafie-Khah, P. Siano, D.Z. Fitiwi, N. Mahmoudi, J.P.S. Catalão, An innovative two-level model for electric vehicle parking lots in distribution systems with renewable energy, IEEE Trans. Smart Grid 9 (2) (Mar. 2018) 1506–1520.
[14] B. Hashemi, M. Shahabi, P. Teimourzadeh-Baboli, Stochastic-based optimal charging strategy for plug-in electric vehicles aggregator under incentive and regulatory policies of DSO, IEEE Trans. Veh. Technol. 68 (4) (Apr. 2019) 3234–3245.
[15] M.W. Tian, S.R. Yan, X.X. Tian, M. Kazemi, S. Nojavan, K. Jermsittiparsert, Risk-involved stochastic scheduling of plug-in electric vehicles aggregator in day-ahead and reserve markets using downside risk constraints method, Sustain. Cities Soc. 55 (April 2020).
[16] M. Amjad, A. Ahmad, M.H. Rehmani, T. Umer, A review of EVs charging: from the perspective of energy optimization, optimization approaches, and charging techniques, Transp. Res. D Transp. Environ. 62 (Jul. 2018) 386–417.
[17] N. Bañol Arias, S. Hashemi, P.B. Andersen, C. Træholt, R. Romero, Distribution system services provided by electric vehicles: recent status, challenges, and future prospects, IEEE Trans. Intell. Transp. Syst. 20 (12) (Dec. 2019) 4277–4296.
[18] M. González Vayá, G. Andersson, Self scheduling of plug-in electric vehicle aggregator to provide balancing services for wind power, IEEE Trans. Sustain. Energy 7 (2) (Apr. 2016) 886–899.
[19] M.H. Abbasi, M. Taki, A. Rajabi, L. Li, J. Zhang, Coordinated operation of electric vehicle charging and wind power generation as a virtual power plant: a multi-stage risk constrained approach, Appl. Energy 239 (Apr. 2019) 1294–1307.
[20] P. Afzali, M. Rashidinejad, A. Abdollahi, A. Bakhshai, Risk-constrained bidding strategy for demand response, green energy resources, and plug-in electric vehicle in a flexible smart grid, IEEE Syst. J. (Mar. 2020) 1–8.
[21] H. Shahinzadeh, J. Moradi, Z. Pourmirza, E. Kabalci, M. Benbouzid, and S.M. Muyeen, "Optimal operation of distributed flexible generation sources incorporating VPP framework in market environment considering uncertainties," in *2022 IEEE Kansas Power Energy Conf. (KPEC)*, April 2022, pp. 1–5.
[22] J. Kim, S.W. Kim, Y.G. Jin, J.-K. Park, Y.T. Yoon, Optimal coordinated management of a plug-in electric vehicle charging station under a flexible penalty contract for voltage security, Energies 9 (7) (Jul. 2016) 538–552.
[23] Y. Liu, H. Liang, A discounted stochastic multiplayer game approach for vehicle-to-grid voltage regulation, IEEE Trans. Veh. Technol. 68 (10) (Oct. 2019) 9647–9659.
[24] B.S.K. Patnam, N.M. Pindoriya, DLMP calculation and congestion minimization with EV aggregator loading in a distribution network using bilevel program, IEEE Syst. J. 15 (2) (June 2021) 1835–1846.
[25] A. Tazikeh Lemeski, R. Ebrahimi, A. Zakariazadeh, Optimal decentralized coordinated operation of electric vehicle aggregators enabling vehicle to grid option using distributed algorithm, J. Energy Storage 54 (Oct. 2022).
[26] H. Ren, A. Zhang, F. Wang, X. Yan, Y. Li, N. Duić, M. Shafie-khah, J.P.S. Catalão, Optimal scheduling of an EV aggregator for demand response considering triple level benefits of three-parties, Int. J. Electr. Power Energy Syst. 125 (Feb. 2021).
[27] C. Feng, Y. Liu, J. Zhang, A taxonomical review on recent artificial intelligence applications to PV integration into power grids, Int. J. Electr. Power Energy Syst. 132 (Nov. 2021).
[28] B. Hashemi, A. Cretu, S. Taheri, Snow loss prediction for photovoltaic farms using computational intelligence techniques, IEEE J. Photovolt. 10 (4) (Jul. 2020) 1044–1052.
[29] E. Lorenz, D. Heinemann, C. Kurz, Local and regional photovoltaic power prediction for large scale grid integration: assessment of a new algorithm for snow detection, Prog. Photovolt., Res. Appl. 20 (6) (Sep. 2012) 760–769.
[30] S. Iyengar, N. Sharma, D. Irwin, P. Shenoy, K. Ramamritham, A cloud-based black-box solar predictor for smart homes, ACM Trans. Cyber-Phys. Syst. 1 (4) (Oct. 2017) 1–24.
[31] F. Wang, Z. Zhang, C. Liu, Y. Yu, S. Pang, N. Duić, et al., Generative adversarial networks and convolutional neural networks based weather classification model for day ahead short-term photovoltaic power forecasting, Energy Convers. Manag. 181 (Feb. 2019) 443–462.
[32] D. Koster, F. Minette, C. Braun, O. O'Nagy, Short-term and regionalized photovoltaic power forecasting, enhanced by reference systems, on the example of Luxembourg, Renew. Energy 132 (Mar. 2019) 455–470.
[33] A. Safdarian, M. Fotuhi-Firuzabad, M. Lehtonen, Integration of price-based demand response in DisCos' short-term decision model, IEEE Trans. Smart Grid 5 (5) (Sep. 2014) 2235–2245.
[34] New York Independent System Operator Inc., Rensselaer, NY, USA. [Online]. Available: http://www.nyiso.com.
[35] Dayton Power and Light Company, Dayton, OH, USA. [Online]. Available: https://www.dpandlpowerauctions.com/LoadData.aspx.
[36] U.S. Local Climatological Data, "National Ocean and Atmospheric Administration" [online] Available: http://www.ncdc.noaa.gov/.
[37] S. Hochreiter, J. Schmidhuber, Long short-term memory, Neural Comput 9 (8) (Nov. 1997) 1735–1780.

[38] "Photovoltaic data acquisition," [online] Available: http://maps.nrel.gov/pvdaq/.
[39] W.H. Kersting, "Radial distribution test feeders," in *Proc. IEEE Power Eng. Soc. Winter Meeting*, Columbus, OH, USA, 2001, pp. 908–912.
[40] Transportation Research Center at Argonne National Laboratory, [online] Available: https://www.anl.gov/es/light-duty-electric-drive-vehicles-monthly-sales-updates.
[41] "Battery Pack Prices Cited Below $100/kWh for the First Time in 2020, While Market Average Sits at $137/kWh," [Online]. Available: https://about.bnef.com/blog/battery-pack-prices-cited-below-100-kwh-for-the-first-time-in-2020-while-market-average-sits-at-137-kwh/.